DOI: 10.1002/anie.201001463

Organic Metals

A Two-Dimensional Organic Metal Based on Fullerene**

Dmitri V. Konarev, Salavat S. Khasanov, Akihiro Otsuka, Mitsuhiko Maesato, Gunzi Saito,* and Rimma N. Lyubovskaya*

We report the synthesis and studies of the physical properties of the first two-dimensional (2D) fullerene organic metal to have 2D layers with a honeycomb arrangement of $C_{60}^{\bullet-}$, $(MDABCO^+)\cdot TPC\cdot(C_{60}^{\bullet-})$ (**1**); we employed a multicomponent and molecular symmetry synthetic approach, starting from the *N*-methyldiazabicyclooctane cation ($MDABCO^+$) and triptycene (TPC). Compound **1** is a fascinating example of a material composed of only light elements (C, H, N) that exhibits a metallic state down to 1.9 K. Salts of fullerene C_{60} with a number of different inorganic cations have previously shown metallic or superconducting properties. Among the fullerene metals, the best known families are MC_{60} salts (M = K, Rb, Cs), which contain linearly polymerized $C_{60}^{\bullet-}$, and superconducting M_3C_{60} salts (M = alkali metals), obtained by doping C_{60} with alkali metals, which have transition temperatures (T_c) of up to 38 K.[1–4] As metal cations expand the three-dimensional (3D) lattice of the initial C_{60} framework, M_3C_{60} salts exhibit 3D metallic conductivity, whereas MC_{60} salts are either 3D (when M = K) or quasi-1D metals (when M = Rb or Cs). 2D fullerene metals have not yet been obtained, whilst the various possible ways of modifying M_xC_{60} salts have almost been exhausted. The idea of obtaining purely organic molecular metals or superconductors from fullerenes has remained unrealized, despite being considered for many years. None of the $C_{60}^{\bullet-}$ salts of organic cations have exhibited metallic properties. The salt $(NMe_4^+)\cdot(C_{60}^{\bullet-})\cdot THF_{1.5}$ showed rather high conductivity, yet was a semiconductor.[5] By synthesizing organic molecular crystals from C_{60} and organic electron donor molecules, it is possible to produce conductors with unique structures and properties.

We have developed a multicomponent approach for synthesizing ionic fullerene compounds that enables the synthesis of ionic fullerene solids $D_I^+\cdot D_{II}\cdot C_{60}^{\bullet-}$ of various structures.[6,7] D_I^+ is a small, strong donor or cation that ionizes C_{60} and determines its charged state, whereas D_{II} is a large, neutral molecule that defines the crystal packing of the complex. In order to exhibit metallic properties, the fullerene sublattice should have a close-packed structure. However, $C_{60}^{\bullet-}$ radical anions have a strong tendency for dimerization, and when they are allowed to approach each other they normally form diamagnetic single-bonded $(C_{60}^-)_2$ dimers.[7–9] In this study, by choosing D_{II} molecules with suitable spatial geometry and size, we were able to synthesize a complex with a close-packed fullerene 2D sublattice in which the $C_{60}^{\bullet-}$ monomers preferentially form a 2D honeycomb network of $C_{60}^{\bullet-}$ rather than undergo dimerization. We expected that TPC (Figure 1), which forms molecular complexes with C_{60},[10,11] would offer a suitable geometrical space and spatial regulation as the D_{II} component for $C_{60}^{\bullet-}$ ions in ionic multicomponent complexes. Indeed, it forms hexagonal layers with voids that accommodate foreign cations, such as $MDABCO^+$ (D_I^+), in the first key–keyhole relationship (Figure 1a). Docking $C_{60}^{\bullet-}$ into the periodic hollow sites in the $(MDABCO^+)\cdot TPC$ network (second key–keyhole relationship; Figure 1a,b) leads to hexagonal packing of the fullerene layers without dimerization of the $C_{60}^{\bullet-}$ monomers.

We used diffusion to obtain good-quality single crystals of complex **1**, which have a rhombohedral structure at 300 K. The $C_{60}^{\bullet-}$ radical anions (the charged state was confirmed spectroscopically)[12] formed uniform hexagonal close-packed layers of two types, *A* and *B*, which alternate with the $(MDABCO^+)\cdot TPC$ layers along the *c* axis (Figure 2a). In type *A* layers, the $C_{60}^{\bullet-}$ radical anions are ordered and packed as shown in Figure 1, with the uncharged nitrogen atoms of the $MDABCO^+$ cations arranged directly above the fullerene hexagons (Figure 2a,b). Layers of type *B* show dynamic disorder of the $C_{60}^{\bullet-}$ anions at 300 K, with methyl groups of $MDABCO^+$ cations slightly penetrating into the periodic hollow sites in the hexagonal packing of disordered $C_{60}^{\bullet-}$ ions (Figure 2a,c).

In both types of layers, each $C_{60}^{\bullet-}$ has six fullerene neighbors with an equal center-to-center distance of 10.073(1) Å at 300 K, which decreases to 9.967(1) Å at 185 K. In type *B* layers, the disorder of $C_{60}^{\bullet-}$ ions at 300 K could be described as flipping between three symmetrically related orientations of $C_{60}^{\bullet-}$ with 1/3 occupancy for each

[*] D. V. Konarev, Prof. R. N. Lyubovskaya
Institute of Problems of Chemical Physics RAS
Chernogolovka, Moscow region, 142432 (Russia)
E-mail: konarev@icp.ac.ru
S. S. Khasanov
Institute of Solid State Physics RAS
Chernogolovka, Moscow region, 142432 (Russia)
A. Otsuka
Research Center for Low Temperature and Materials Sciences
Kyoto University, Sakyo-ku, Kyoto 606-8501 (Japan)
M. Maesato
Division of Chemistry, Graduate School of Science
Kyoto University, Sakyo-ku, Kyoto 606-8502 (Japan)
Prof. G. Saito
Research Institute, Meijo University
1-501 Shiogamaguchi, Tempaku-ku, Nagoya 468-8502 (Japan)
E-mail: gsaito@ccmfs.meijo-u.ac.jp

[**] This work was supported by a Grant-in-Aid for Scientific Research from MEXT, Japan (152005019, 21st Century COE 15073215, and 20110006), JSPS (18GS0208), RFBR(grant N 09-02-01514), Japan–Russia Bilateral Joint Research Program by JSPS, and The Sumitomo Foundation. We thank C. Michioka and M. Sakata for their technical assistance in physical property experiments.

Supporting information for this article is available on the WWW under http://dx.doi.org/10.1002/anie.201001463.

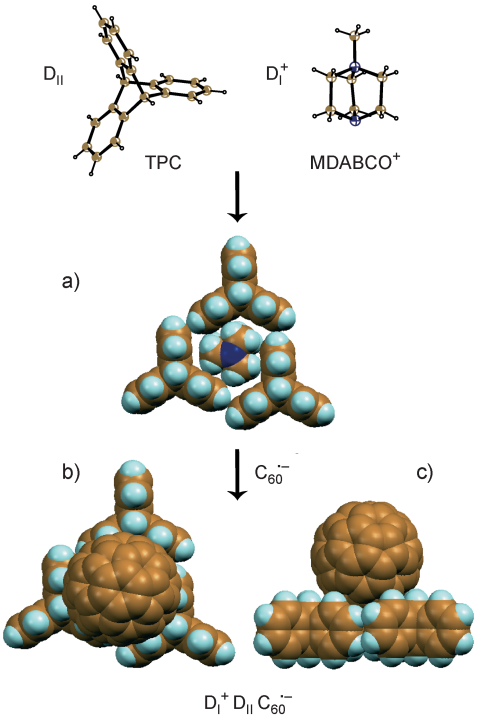

Figure 1. Molecular structures of TPC (D_{II}) and MDABCO$^+$ (D_I^+). a) Crystal structure packing in **1**; TPC molecules form a hexagonal hollow in which the MDABCO$^+$ cation fits. b,c) Two orthogonal views of $D_I^+D_{II}C_{60}^{\bullet-}$ that show $C_{60}^{\bullet-}$ molecules docked in the hollow in the TPC layer in a key–keyhole relationship. Colors: C dark yellow, H pale blue, N dark blue.

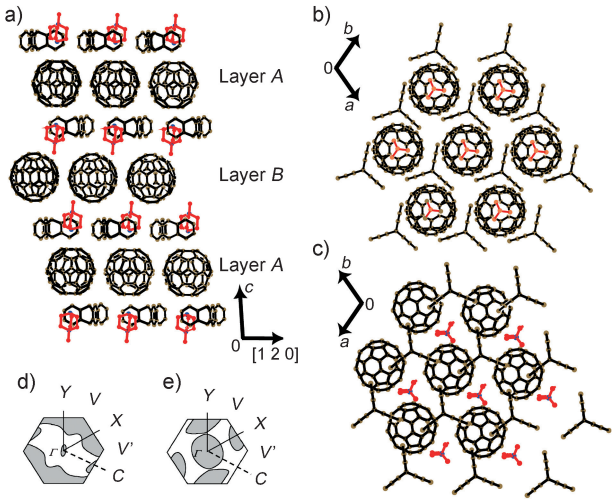

Figure 2. Crystal structure of **1** at 160 K: a) Projection along the [100] axis. b) Projection of the (MDABCO$^+$)·TPC layer on the C_{60} layer *A*; c) projection of the (MDABCO$^+$)·TPC layer on the C_{60} layer *B*. At 300 K, $C_{60}^{\bullet-}$ in layer *B* and half of the MDABCO$^+$ cations are rotating. MDABCO$^+$ cations are indicated by the red color. Calculated Fermi surface of **1** at 160 K in d) layer *A* and e) layer *B*.

orientation. At the same temperature, half of the MDABCO$^+$ cations are disordered between three orientations, linked by their rotations about the lattice threefold axis. Ordering of the orientations of $C_{60}^{\bullet-}$ and MDABCO$^+$ was observed once the temperature dropped below 200 K, followed by a structural transition into a triclinic unit cell below 183 K, and finally by a complete ordering of all three component molecules in the crystal structure at 160 K (Figure 2a). These observations suggest that the orientation disorder of $C_{60}^{\bullet-}$ is closely linked with that of MDABCO$^+$. The environmental difference between layers *A* and *B* imparts intriguing transport and magnetic behaviors, as shown below. An abnormal hump in the graph of specific heat versus temperature between 210 and 180 K was observed; the sharp peak at 198 K (Figure 3a) may correspond to a freezing of the rotational degrees of freedom of $C_{60}^{\bullet-}$ and MDABCO$^+$. At the structural transition below 183 K, the center-to-center distances along the [100] and [110] axes became shorter (9.909(1) and 9.923(1) Å, respectively), while the distance along the [010] axis increased slightly (10.022(2) Å), thus resulting in a slight asymmetry in the fullerene layers *A* and *B* at 160 K.

We calculated the 2D closed Fermi surfaces (FSs) using a tight-binding method with AM1 calculations based on the crystal structures for layer *A* at 185, 200, 240, and 300 K. Point contact interactions between the spherical $C_{60}^{\bullet-}$ radical anions led to narrow bandwidths (0.103–0.150 eV). Calculation of FSs at 160 K for both layers (Figure 2d,e) showed that anisotropy in the layers increased below 183 K, but the FSs retained its 2D character, thus suggesting that the compound remained metallic at that temperature.

The salt is highly conductive, and showed a metallic temperature dependence within the *ab* plane from 360 K (0.57 Ω cm) to 200 K (0.07 Ω cm), followed by a steep decrease in resistivity from 200 to 185 K (0.03 Ω cm; Figure 3b). The temperature of this anomaly coincided well with that of an ordering of the $C_{60}^{\bullet-}$ ions in layer *B*, thus indicating that the ordered $C_{60}^{\bullet-}$ radical anions in layer *B* start to participate in metallic transport below 200 K. The resistivity decreased slowly from 183 down to 160 K and then increased slightly as the temperature was lowered to 70 K. The resistivity below 70 K could not be accurately measured because of a large increase in the contact resistance. It seems that the structural transition (rhombohedral to triclinic) interrupts the metallic behavior of the crystal because of an increase in the anisotropy of the electronic structure and the formation of twining domains that have three possible orientations. The interlayer resistivity, which shows almost-temperature-independent behavior above 200 K, is 10^2–10^3 times larger than the intralayer resistivity (Figure 3b). The large anisotropy in resistance reflects the highly 2D nature of **1**.

With a microwave electric field oriented parallel to the conducting fullerene layers, *E*//*ab*, the electron paramagnetic resonance (EPR) spectra of single crystals shows a signal with $g = 1.9973$ and a linewidth (ΔH) of 3.33 mT (300 K), which is ascribed to $C_{60}^{\bullet-}$.[6,9,13] The signal has an asymmetric Dysonian shape that is characteristic of highly conductive materials (Figure 3c, inset). Such EPR signals have been previously observed in 2D organic metals and superconductors that were based on bis(ethylenedithio)tetrathiafulvalene (ET), such as [β-$(ET)_2I_3$],[14] but here they are observed for the first time in fullerene-based metals. The asymmetry ratio between the

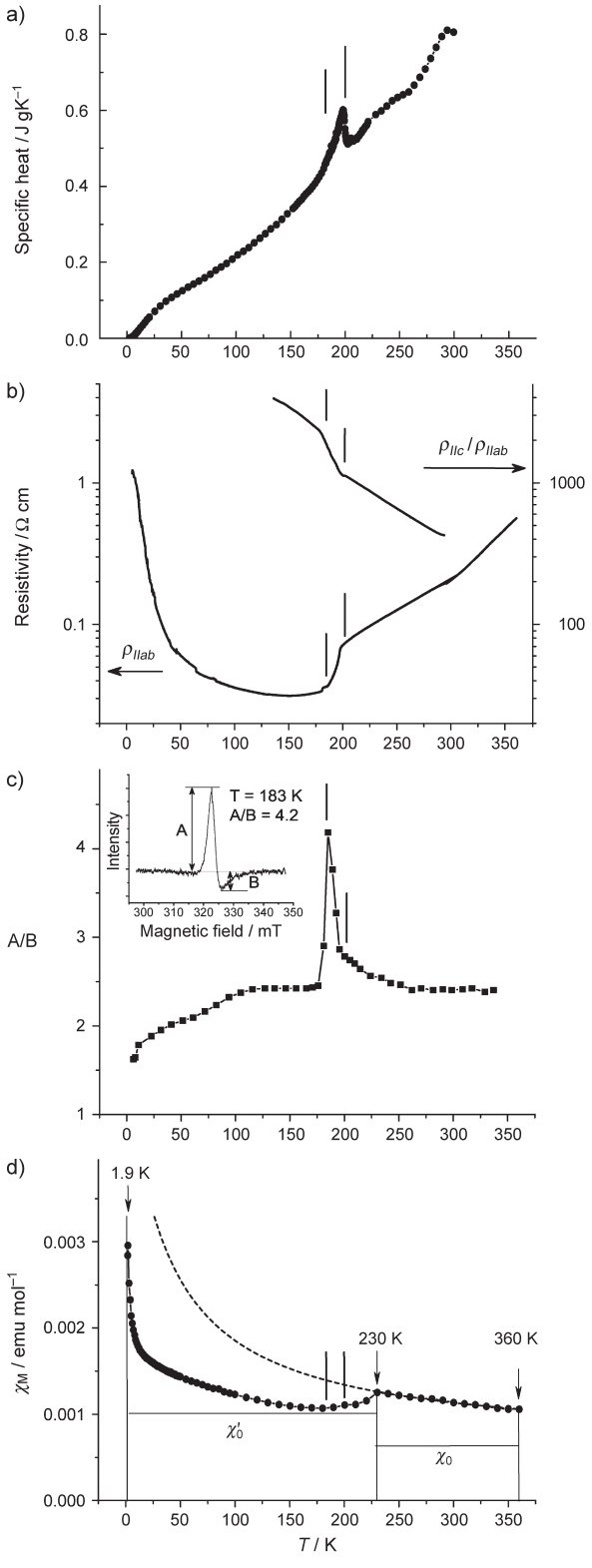

Figure 3. a) The specific heat of **1** as a function of temperature; b) the temperature dependence of intralayer resistivity ($\rho \| ab$) and the $\rho \| c/\rho \| ab$ ratio of a single crystal of **1**; c) the temperature dependence of A/B for the Dysonian EPR line from the oriented single crystal (inset shows the spectrum at 183 K); d) the temperature dependence of the molar magnetic susceptibility (χ_M/ emu mol^{-1}) of **1** (closed circles). Dashed curve fits to $\chi_0 + C/(T-\Theta)$, where $\chi_0 = 6.5\times10^{-4}$ emu mol^{-1}, $C = 0.160$ emu K mol^{-1}, and $\Theta = -31$ K. Two vertical bars in all the figures indicate the temperature interval from 200 to 185 K.

maxima and minima of the absorption derivative (A/B) is 2.4 at 300 K. A/B exhibits an abrupt increase as the temperature drops below 200 K, reaching a maximum of 4.2 at 183 K (Figure 3c), which corresponds well with the increase in conductivity; the asymmetry ratio then falls to 2.3 at temperatures below 183 K. A/B slowly decreases with temperature, but the Dysonian shape of the EPR signal is still observed, even at 4 K (A/B = 1.64), thus confirming the existence of a highly conducting state at temperatures down to 4 K.

Magnetic measurements were performed using a SQUID magnetometer in the 1.9–360 K range for a collection of single crystals. Over the range 230–360 K, the molar magnetic susceptibility (χ_M) can be fitted to a combination of the Pauli and Curie–Weiss terms ($\chi_M = \chi_0 + C/(T-\Theta)$ with a constant $\chi_0 = 6.5\times10^{-4}$ emu mol^{-1}, $C = 0.160$ emu K mol^{-1}, and $\Theta = -31$ K; Figure 3d, dashed curve). The C value of 0.160 emu K mol^{-1} corresponds to the contribution of about 50% of the spins from the total amount of C_{60} ($C = 0.374$ emu K mol^{-1} for 100% of spins). Considering the presence of different types of C_{60} layers in **1**, i.e. *A* and *B*, it is likely that the spins in one layer are localized and interact antiferromagnetically with a Θ of −31 K. The Pauli paramagnetic contribution χ_0 is attributable to the conducting electrons of another metallic fullerene layer. A reversible decrease in magnetic susceptibility (χ_M) is observed at 230–200 K. Below 200 K, the temperature-independent susceptibility (χ'_0) of about 10.0×10^{-4} emu mol^{-1} can be attributed to the Pauli paramagnetic contribution of both metallic fullerene layers, which implies that **1** has a metallic state down to 1.9 K. The Curie tail at low temperatures corresponds to a contribution of less than 1.2% of spins from the total amount of C_{60}. The reversible decrease in χ_M at 230–200 K is accompanied by a gradual increase in A/B (Figure 3c), followed by an abrupt increase in A/B and conductivity below 200 K (Figure 3c,b), which corresponds to the order–disorder transition of $C_{60}^{\bullet-}$ in type *B* layers. Therefore, the most plausible explanation is that ordering of $C_{60}^{\bullet-}$ in the type *B* layers with $MDABCO^+$ triggers a transition from a nonmetallic and antiferromagnetically frustrated state to a metallic state in layer *B*, whilst the ordered $C_{60}^{\bullet-}$ in layer *A* kept its 2D itinerancy over the entire temperature range. The strong correlation between the ordering of C_{60} and the physical properties of **1** is intriguing, and was previously observed in some fullerene salts.[15–18]

To summarize, we synthesized single crystals of the first fullerene-based 2D organic metal ($MDABCO^{+)}\cdot TPC\cdot(C_{60}^{\bullet-})$ (**1**) in which fullerene radical anions are closely packed in a hexagonal 2D array. **1** is the first 2D metal among the reported fullerene conductors, and it exhibits a metallic state down to 1.9 K, which can be explained by the 2D character of the electronic structure. Quasi-1D metals MC_{60} (M = Rb and Cs) undergo transitions into the insulating state below 50 and 40 K, respectively.[1] Our technique has significant potential for producing new materials by the changing the D_I^+ and D_{II} components in **1**. As the close-packed fullerenes form a 2D triangular lattice, exotic electronic states, such as superconductivity and spin-liquid states,[19] might be realized in materials based on fullerenes that are produced using our method.

Experimental Section

The preparation of $(MDABCO^+)\cdot TPC\cdot(C_{60}^{\bullet-})$ (**1**): C_{60} (25 mg) was stirred with a tenfold molar excess of CH_3CH_2SNa and a fivefold molar excess of MDABCOI in $C_6H_4Cl_2/C_6H_5CN$ solution (14 mL/2 mL). TPC (160 mg) was dissolved in the resulting mixture, and the solution was cooled and filtered in a glass tube. Hexane (25 mL) was layered on top of the solution, and the diffusion was performed over 2 months, producing black hexagonal prisms of **1** on the walls of the tube (yield 50–60%).

Crystal data for **1**: $C_{174}H_{58}N_4$, MW = 2204.24, black prism, 0.5 × 0.4 × 0.3 mm. 300(2) K: rhombohedral, space group $R\bar{3}$: h, a = 10.0722(5), b = 10.0722(5), c = 83.989(4) Å, V = 7291.2(6) Å^3, Z = 3, d_{calcd} = 1.506 Mg m^{-3}, μ = 0.087 mm^{-1}, $2\theta_{max}$ = 54.40°; 9243 reflections collected, 3591 independent; R_1 = 0.0508 for 2888 observed data [$>2\sigma(F)$] with 2889 restraints and 517 parameters; wR_2 = 0.1529 (all data); final GoF = 1.043.

200(2) K: rhombohedral, space group $R\bar{3}$: h, a = 9.9850(5), b = 9.9850(5), c = 83.344(4) Å, V = 7196.1(6) Å^3, Z = 3, d_{calcd} = 1.526 Mg m^{-3}, μ = 0.088 mm^{-1}, $2\theta_{max}$ = 54.78°; 8811 reflections collected, 3517 independent; R_1 = 0.0453 for 2980 observed data [$>2\sigma(F)$] with 2889 restraints and 517 parameters; wR_2 = 0.1197 (all data); final GoF = 1.039.

185(2) K: rhombohedral, space group $R\bar{1}$: h, a = 9.9670(10), b = 9.9670(10), c = 83.379(8) Å, V = 7173.3(12) Å^3, Z = 3, d_{calcd} = 1.531 Mg m^{-3}, μ = 0.088 mm^{-1}, $2\theta_{max}$ = 55.00°; 19291 reflections collected, 10225 independent; R_1 = 0.0580 for 6348 observed data [$>2\sigma(F)$] with 10869 restraints and 1434 parameters; wR_2 = 0.1586 (all data); final GoF = 0.993.

160(2) K: triclinic, space group $P\bar{1}$, a = 9.9090(10), b = 10.0218(8), c = 28.3711(19) Å, α = 99.677(3), β = 91.217(2), γ = 120.284(18)°, V = 2379.7(3) Å^3, Z = 1, d_{calcd} = 1.538 Mg m^{-3}, μ = 0.089 mm^{-1}, $2\theta_{max}$ = 54.64°; 14841 reflections collected, 7948 independent; R_1 = 0.0449 for 6485 observed data [$>2\sigma(F)$] with 2577 restraints and 805 parameters; wR_2 = 0.1037 (all data); final GoF = 1.051.

X-ray diffraction data for **1** at 160, 185, 200, and 300 K were collected on a MAC Science DIP-2020 K oscillator type X-ray imaging plate diffractometer with graphite-monochromated $Mo_{K\alpha}$ radiation using an Oxford Cryostream cooling system. The structures were solved by direct methods and refined by the full-matrix least-squares method against F^2 using SHELX-97 (G. M. Sheldrick).

Received: March 11, 2010
Revised: April 2, 2010
Published online: June 8, 2010

Keywords: conducting materials · crystal engineering · fullerenes · layered compounds · magnetic properties

[1] F. Bommeli, L. Degiorgi, D. Wachter, Ö. Legeza, A. Jánossy, G. Oszlanyi, O. Chauvet, L. Forro, *Phys. Rev. B* **1995**, *51*, 14794–14797.
[2] A. F. Hebard, M. J. Rosseinsky, R. C. Haddon, D. W. Murphy, S. H. Glarum, T. T. M. Palstra, A. P. Ramirez, A. R. Kortan, *Nature* **1991**, *350*, 600–601.
[3] M. J. Rosseinsky, *J. Mater. Chem.* **1995**, *5*, 1497–1513.
[4] A. Y. Ganin, Y. Takabayashi, Y. Z. Khimyak, S. Margadonna, A. Tamai, M. J. Rosseinsky, K. Prassides, *Nat. Mater.* **2008**, *7*, 367–371.
[5] R. E. Douthwaite, M. A. Green, M. L. H. Green, M. J. Rosseinsky, *J. Mater. Chem.* **1996**, *6*, 1913–1920.
[6] D. V. Konarev, S. S. Khasanov, R. N. Lyubovskaya, *Russ. Chem. Bull.* **2007**, *56*, 371–392.
[7] D. V. Konarev, S. S. Khasanov, G. Saito, A. Otsuka, R. N. Lyubovskaya, *J. Mater. Chem.* **2007**, *17*, 4171–4177.
[8] D. V. Konarev, S. S. Khasanov, A. Otsuka, G. Saito, *J. Am. Chem. Soc.* **2002**, *124*, 8520–8521.
[9] D. V. Konarev, S. S. Khasanov, G. Saito, A. Otsuka, Y. Yoshida, R. N. Lyubovskaya, *J. Am. Chem. Soc.* **2003**, *125*, 10074–10083.
[10] D. V. Konarev, Yu. V. Zubavichus, E. F. Valeev, Yu. L. Slovokhotov, Yu. M. Shul'ga, R. N. Lyubovskaya, *Synth. Met.* **1999**, *103*, 2364–2365.
[11] E. M. Veen, P. M. Postma, H. T. Jonkman, A. L. Spek, B. L. Feringa, *Chem. Commun.* **1999**, 1709–1710.
[12] Optical data indicate that fullerenes in both layers *A* and *B* have an approximately equal −1 charge on the molecule. The $F_{1u}(4)$ mode of C_{60}, which is most sensitive to its charged state, is positioned as a single unsplit line at 1386 cm^{-1}. The absorption bands of neutral C_{60} at 1429 cm^{-1} or C_{60}^{2-} dianions at 1369 cm^{-1} are absent in the spectrum. The NIR spectrum is also characteristic of the $C_{60}^{\bullet-}$ radical anions.
[13] P. M. Allemand, G. Srdanov, A. Koch, K. Khemani, F. Wudl, Y. Rubin, F. Diederich, M. M. Alvarez, S. J. Anz, R. L. Whetten, *J. Am. Chem. Soc.* **1991**, *113*, 2780–2781.
[14] T. Sugano, G. Saito, M. Kinoshita, *Phys. Rev. B* **1986**, *34*, 117–125.
[15] T. Yildirim, J. E. Fischer, A. B. Harris, P. W. Stephens, D. Liu, L. Brard, R. M. Strongin, A. B. Smith III, *Phys. Rev. Lett.* **1993**, *71*, 1383–1386.
[16] K. Prassides, C. Christides, I. M. Thomas, J. Mizuki, K. Tanigaki, I. Hirosawa, T. W. Ebbesen, *Science* **1994**, *263*, 950–954.
[17] D. Mihailovic, D. Arcon, P. Verturini, R. Blinc, A. Omerzu, P. Cevc, *Science* **1995**, *268*, 400–402.
[18] M. Akada, T. Yamamoto, R. Kumashiro, A. Hojvo, H. Matsui, N. Toyota, J. P. Lu, K. Tanigaki in *Multifunctional conducting molecular materials* (Eds.: G. Saito, et al.), The Royal Society of Chemistry, Cambridge, UK, **2007**, pp. 191–197.
[19] Y. Shimizu, K. Miyagawa, K. Kanoda, M. Maesato, G. Saito, *Phys. Rev. Lett.* **2003**, *91*, 107001.
[20] CCDC 768376 (**1**), CCDC 768378 (200 K), CCDC 768379 (185 K), and CCDC 768380 (160 K) contain the supplementary crystallographic data for this paper. These data can be obtained free of charge from The Cambridge Crystallographic Data Centre via www.ccdc.cam.ac.uk/data_request/cif.

